DESIGN OF SPLIT-RING RESONATOR BANDPASS FILTER FOR MOBILE COMMUNICATIONS

Barol Léonard Mafouma Kiminou, Nzonzolo, Franck Moukanda Mbango, Lionel Nkounka Moukengue, Désiré Lilonga-Boyenga
Laboratory of Electrical and Electronics Engineering,
Ecole Nationale Supérieure Polytechnique,
Université Marien NGouabi Brazzaville – CONGO

ABSTRACT
A bandpass split ring resonators filter is proposed for the mobile communications. This filter functioning between 0.94 and 1.06 GHz is realized in microstrip technology with split ring resonators with a inside hairpin structure with an aim obtaining the compact filter with small size, less weight and small length. This planar filter presents improved performances in particular in terms of the insertion loss less than those of the traditional resonator filters.

Keywords: Resonator, Coupling Matrix, Split Ring, Quadruplet.

1. INTRODUCTION

The split ring resonator (SRR) was suggested for the first time in 1999 by Pendry for the characterization of metamaterials [1]. It was proposed also later in 1997 by Miyake and 2006 by Garcia-Lamperez as resonators for microstrip bandpass filters, because of its small size, its low cost and the improved performance of the filters they bring [2]. In 2017, Z. Troudi proposed a new optimized RSS structure with twisted arms more efficient than the classic square SRR, especially in terms of miniaturization and low insertion losses [3].
Several studies have been conducted on split ring resonators in 2018, indeed, Armando Fernández-Prieto proposed a compact diplexer designed with two balanced bandpass filters using split ring resonators. The use of magnetic coupling reduces signal transmission and the use of capacitive coupling leads to a very compact design of the structure [4]. R. Sushmeetha proposed an equivalent circuit model of the dual-band bandpass filter with complementary split-ring resonators. By varying the length and width of the resonators and changing the width of the microstrip line, the desired resonant frequencies are obtained [5]. Mohammed Bendaoued in 2019 worked on the low-pass filter with square split ring resonators in order to suppress the spurious response and to have a good rejection in the stopband [6]. More recently, Mohssine El Ouahobi has proposed a compact dual band filter using a network of square ring resonators, grounded to cut off the unwanted signals [7].

The SRR have lower resonance frequencies. They offer better selectivity and better reduction of insertion losses than conventional open loop resonators of the same size. Because of the strong interaction between the two constituent ring conductors, each RSS behaves as a pair of over-coupled resonators with two different resonances [8].

In this work, we will focus on the split ring resonators using inside a hairpin resonator that ends with two parallel lines coupled in order to reduce the insertion losses observed on the classic square RSS filter. The synthesis of filters based on split ring resonators will take place in two stages: firstly, the search for the coupling matrix from the rational polynomials coefficients of transfer and reflection parameters S_{21} and S_{11}, and secondly, the determination of the electrical, magnetic and mixed couplings from electromagnetic simulations made on two resonators depending on the distance between them.

2. THEORETICAL APPROACH

Let us consider a network of coupled resonators whose equivalent circuit consisting of n loops as shown in Figure 1, fed by a R_1 resistance source and charged by an R_N resistance. The synthesis of filters based on such a network was first introduced by Atia [9] and later generalized by R. Cameron [10]. The synthesis procedure of resonators coupled filter involves the determination of the coupling matrix between resonators from the transfer and reflection polynomials and was largely established by [10].
The starting point for the synthesis of the network coupling matrix is the determination of the transfer and reflection polynomials defined by [11]:

$$S_{21}(s) = \frac{\mathrm{P(s)}}{\varepsilon \mathrm{E(s)}} \quad \text{et} \quad S_{11}(s) = \frac{\mathrm{F(s)}}{\varepsilon_R \mathrm{E(s)}} \qquad (1)$$

$P(s)$ and $F(s)$ represent respectively the numerators of the transfer and reflection coefficients and E(s), their common denominator in the complex plane s, ε and ε_R , the ripple level coefficient of transfer and reflection in the bandwidth.

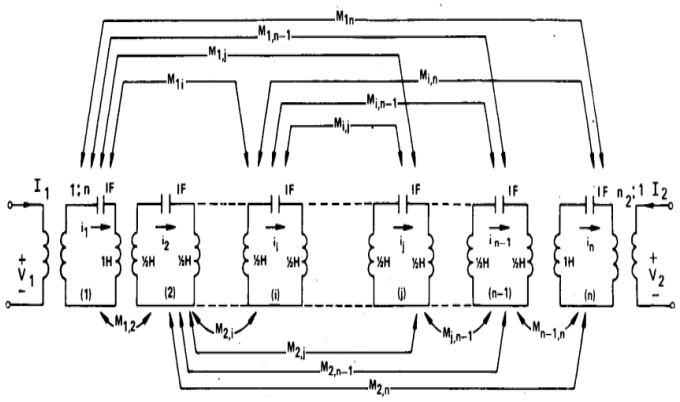

Figure.1: Cross-coupled resonators network

1.1. Determination of transfer and output admittances

The loop equation applying in each resonator of above network leads to the follow relationship between the voltages and currents:

$$[e]^t = [z][i]^t \tag{2}$$

Where $[e] = e[1,0,\ldots.,0]$, $[i] = [\mathrm{i}_1,\ i_2, \ldots,\ i_N]$ and $[Z]$, the overall impedance matrix of the circuit which has as expression:

$$[Z] = [R] + s[I] + j[M] \tag{3}$$

with

$$[R] = \begin{bmatrix} R_1 & 0 & \ldots & 0 \\ 0 & 0 & \ldots & 0 \\ \vdots & \vdots & \ddots & \vdots \\ 0 & 0 & \ldots & R_N \end{bmatrix} ;\ [M] = \begin{bmatrix} M_{11} & M_{12} & \ldots & M_{1N} \\ M_{12} & M_{22} & \ldots & M_{2N} \\ \vdots & \vdots & \ddots & \vdots \\ M_{1N} & M_{2N} & \ldots & M_{NN} \end{bmatrix} \tag{4}$$

[M] is a reciprocal NxN matrix, and [I], the identity matrix.

To obtain a short-circuit coupled resonator network working, it suffices to set $R_1 = R_N = 0$ (that is to say R = 0) in equation (2). Under these conditions, the current vector $[i]$ is given by:

$$[i]^{\mathrm{t}} = [\mathrm{jM} + \mathrm{sI}]^{-1}.[e]^{\mathrm{t}} \tag{5}$$

The exponent t indicates the transposed.

It is immediately apparent that the short-circuit transfer and output admittances have expressions [8]:

$$y_{21}(s) = \frac{i_N}{e_1}\Big|_{R_1 R_N = 0} = [\mathrm{jM} + \mathrm{sI}]^{-1}_{N1} \quad \text{and}$$

$$y_{22}(s) = \frac{i_N}{e_N}\Big|_{R_1 R_N = 0} = [\mathrm{jM} + \mathrm{sI}]^{-1}_{NN} \tag{6}$$

The coupling matrix [M] being real and symmetrical, all its eigenvalues are real. Thus, there exists an orthogonal NxN matrix [T], formed by its eigenvectors, which satisfies the relation:

$$-M = T.\Lambda.T^t \tag{7}$$

where $\Lambda = diag[\lambda_1, \lambda_2, \ldots, \lambda_N]$ is a diagonal eigenvalues matrix of the matrix [M] and $[T]^t$ is the transpose of [T]. The quantity $[\mathrm{jM} + \mathrm{sI}]^{-1}$ can be written:

$$[\mathrm{jM} + \mathrm{sI}]^{-1} = [-jT.\Lambda.T^t + \mathrm{sI}]^{-1} = Tdiad\left[\frac{1}{s-j\lambda_1}, \ldots, \frac{1}{s-j\lambda_n}\right]T^t \tag{8}$$

or

$$[\mathrm{jM} + \mathrm{sI}]^{-1}_{\mathrm{ij}} = \sum_{\mathrm{k}=1}^{\mathrm{N}} \frac{\mathrm{T_{ik}T_{jk}}}{\mathrm{s-j\lambda_k}} , \quad i,j = 1,2,3 \ldots N \tag{9}$$

Substituting the relation (8) in (5), we have:

$$y_{21}(s) = \sum_{k=1}^{n} \frac{T_{1k}T_{Nk}}{s-j\lambda_k} \text{ et } y_{22}(s) = \sum_{k=1}^{n} \frac{T_{Nk}^2}{s-j\lambda_k} \quad (10)$$

Here, T_{ik} and T_{Nk} are the elements of the first and the last row of the orthogonal matrix [T]. These two rows must be orthogonal.

1.2. Synthesis of the admittance matrix [Y_N]

To synthesize the short-circuit admittance matrix [Y_N], we have to determine its elements from the rational polynomials coefficients of the transfer and reflection parameters $S_{21}(s)$ and $S_{11}(s)$ which represent the characteristics of the filter to be realized. [10]. For a two-port, fed by an internal impedance source of 1Ω and loaded by a resistor of 1Ω, the parameters $y_{21}(s)$ and $y_{22}(s)$, for a Chebyshev II filtering function, can be in the form:

$$y_{22}(s) = \frac{y_{22n}(s)}{y_d(s)} = \frac{m_1}{n_1} \quad (12)$$

$$y_{21}(s) = \frac{y_{21n}(s)}{y_d(s)} = {P(s)}/{\varepsilon n_1} \quad (13)$$

where m_1 and n_1 are two polynomials in s which make it possible to write the denominator of $S_{21}(s)$ and $S_{11}(s)$ in the form:

$E(s) = m_1 + n_1$
with
$m_1 = R_e(e_0 + f_0) + jIm(e_1 + f_1)s + R_e(e_2 + f_2)s^2 + \cdots$
$n_1 = jIm(e_0 + f_0) + R_e(e_1 + f_1)s + jIm(e_2 + f_2)s^2 + \cdots$ (14)
where $i = 0,1,2,3 \ldots N$ for a filter of N order , e_1 and f_i, the complex coefficients.
The process introduced here can guarantee that the polynomials m_1 and n_1 will have alternately real or imaginary coefficients, Since the coefficients of s^N in E (s) and F (s) are equal to 1.
knowing the residues of y_{21} and y_{22}, one can put the admittance matrix [Y_N] of the whole network in the following form:

$$[Y_N] = \begin{bmatrix} 0 & jK_\infty \\ jK_\infty & 0 \end{bmatrix} + \sum_{k=1}^{n} \frac{1}{s-j\lambda_k} \begin{bmatrix} r_{11k} & r_{12k} \\ r_{21k} & r_{22k} \end{bmatrix} \quad (15)$$

where the real constant $K_\infty = 0$, except for the fully canonical case where the number of finite-position zeros (n_{fz}) in the filter function is equal to the degree of the filter N. In this case, the degree of the numerator of $y_{21}(s)$ ($y_{21n}(s) = y_d(s)$) is equal to that of its denominator $y_d(s)$, and $K_\infty \neq 0$. It is calculated from $y_{21}(s)$ to reduce the degree of the numerator $y_{21n}(s)$ before finding the residues r_{21k} [12].

1.3. Synthesis of the coupling matrix [M] of an N+2 transverse network

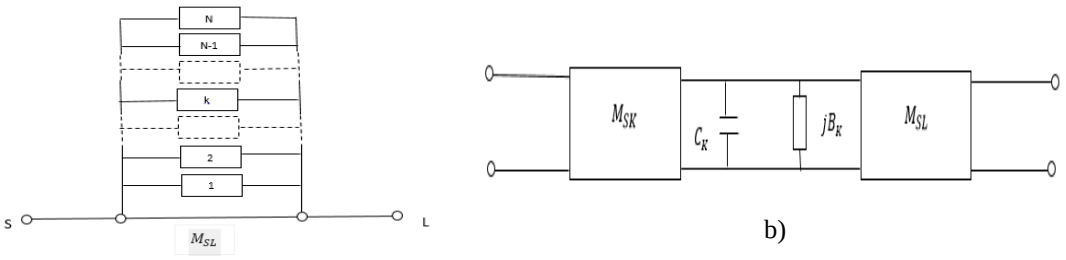

Figure.: Canonical transversal array a) N-resonators transversal array including direct source-load coupling $M_{SL,}$ b) Equivalent circuit of the kth "low-pass resonator" in the transversal array.

In most cases, the synthesis of coupled resonator filters is done from an N+2 cross-network, as shown in Figure 2b. The [ABCD] matrix of the kth resonator of order N is given by [11].

$$[ABCD]_k = -\begin{bmatrix} \frac{M_{Lk}}{M_{Sk}} & \frac{sC_k + jB_k}{M_{Sk}M_{Lk}} \\ 0 & \frac{M_{Sk}}{M_{Lk}} \end{bmatrix} \quad (16)$$

From this [ABCD] matrix, one can deduce the admittance matrix parameters of the circuit:

$$[Y_N] = j\begin{bmatrix} 0 & M_{SL} \\ M_{SL} & 0 \end{bmatrix} + \sum_{k=1}^{N}[y_k] \quad (17)$$

Where

$$[y_k] = \frac{1}{(sC_k+jB_k)}\begin{bmatrix} M_{Sk}^2 & M_{Sk}M_{Lk} \\ M_{Sk}M_{Lk} & M_{Lk}^2 \end{bmatrix} \quad (18)$$

From the comparison of the relations (15) and (17) giving the expressions of the matrix $[Y_N]$, we deduce that:

$$\begin{cases} M_{SL} = K_\infty \\ \frac{r_{21k}}{(s-j\lambda_k)} = \frac{M_{Sk}M_{Lk}}{(sC_k+jB_k)} \\ \frac{r_{22k}}{(s-j\lambda_k)} = \frac{M_{Lk}^2}{(sC_k+jB_k)} \end{cases} \quad (19)$$

The residuals r_{21k} and r_{22k} and the eigenvalues λ_k have already been obtained from the polynomials $S_{21}(s)$ and $S_{22}(s)$ of the desired filtering function and thus by equalizing the real and imaginary parts of the equations 17, it is possible to directly obtain the coupling coefficients between the different resonators [11].

$$\begin{cases} C_k = 1,\ B_k(\equiv M_{kk}) = -\lambda_k;\ M_{Lk}^2 = r_{22k},\ M_{Sk}M_{Lk} = r_{12k}\ ; \\ M_{Lk} = \sqrt{r_{22k}}\ \ et\ \ M_{Sk} = \frac{r_{21k}}{\sqrt{r_{22k}}} \qquad k = 1,2 \ldots N \end{cases} \quad (20)$$

3. Application: split ring resonators bandpass filter design

We propose to design, using the quasi-elliptic approximation, a slit ring resonators bandpass filter on a microstrip structure with four poles and two transmissions zeros $s = \pm 1.4j$, with a central frequency $f_C = 1\ GHz$, a relative bandwidth FWB = 0.05 and reflection losses of 20 dB in the bandwidth.

Taking into account these specifications, we determined the following coupling matrix between the different resonators using a computer code, which we developed in MATLAB software.

$$[M_0] = \begin{bmatrix} 0 & -0.3046 & 0.3046 & 0.6477 & -0.6477 & 0 \\ -0.3046 & 1.2273 & 0 & 0 & 0 & 0.3046 \\ 0.3046 & 0 & -1.2273 & 0 & 0 & 0.3046 \\ 0.6477 & 0 & 0 & 0.7947 & 0 & 0.6477 \\ -0.6477 & 0 & 0 & 0 & -0.7947 & 0.6477 \\ 0 & 0.3046 & 0.3046 & 0.6476 & 0.6476 & 0 \end{bmatrix}$$

It is clear that this matrix is symmetrical with respect to the main diagonal on the one hand and does not allow to achieve without bulk the different couplings between resonators on the other hand. To do this, the technique used consists in making rotations to eliminate certain couplings in order to obtain a simple canonical form of the coupling matrix M and thus a more practical configuration of the circuit to be produced as shown in Figure 3

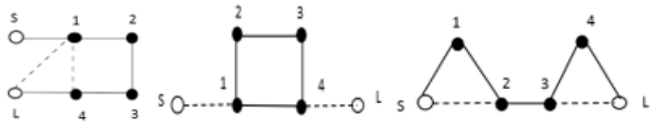

a) b) c)

Figure. 3: Diagram of coupling and rotation: a) for the routing schematic b) for the quadruplet in cascade CQ c) for the trisection

In our case, we chose the quadruplet configuration (Fig.3b). Table I below, gives the pivots and rotation angles for transforming the coupling matrix of the transverse network to the folded configuration. The total number of rotations is here six.

Table 1: Pivots and angles of the similarity transform sequence for the reduction of the transversal matrix to the folded configuration

Transform Number r	Pivot [i,j]	Elément to be annihilated	Figure 3	$\theta_r = \tan^{-1}(cM_{lk}/M_{mn})$				
				k	l	m	n	c
1	[3;4]	M_{S4}	In row S	S	4	S	3	-1
2	[2;3]	M_{S3}		S	3	S	2	-1
3	[1;2]	M_{S2}		S	2	S	1	-1
4	[2;3]	M_{2L}	In	2	L	3	L	+1
5	[3;4]	M_{3L}	Column L	3	L	4	L	+1
6	[2;3]	M_{13}	In row 1	1	3	1	2	-1

After all rotations, we obtain the following coupling matrix of the folded network of the normalized filter

$$[M] = \begin{bmatrix} 0 & 1.0122 & 0 & 0 & 0 & 0 \\ 1.0122 & 0 & 0.7787 & 0 & -0.4285 & 0 \\ 0 & 0.7787 & 0 & 0.8611 & 0 & 0 \\ 0 & 0 & 0.8611 & 0 & 0.7787 & 0 \\ 0 & -0.4285 & 0 & 0.7787 & 0 & 1.0121 \\ 0 & 0 & 0 & 0 & 1.0212 & 0 \end{bmatrix}$$

To obtain the performance of the actual filter, it is necessary to use the de-normalized coupling matrix. For this, we multiply the Mij (j≠i) by the bandwidth. The input/output couplings are obtained by inverting the elements M_{S1} and M_{L4} multiplied by the bandwidth. Thus, the expression of the coupling matrix of the filter is written:

$$[M] = \begin{bmatrix} 0 & 19.7589 & 0 & 0 & 0 & 0 \\ 19.7589 & 0 & 0.0389 & 0 & -0.0214 & 0 \\ 0 & 0.0389 & 0 & 0.0431 & 0 & 0 \\ 0 & 0 & 0.0431 & 0 & 0.0389 & 0 \\ 0 & -0.0214 & 0 & 0.0389 & 0 & 19.7589 \\ 0 & 0 & 0 & 0 & 19.7589 & 0 \end{bmatrix}$$

3.1. Filter realization

We propose to realize this filter with split ring resonators with inside a hairpin structure (Figure 4) on a substrate of thickness h = 1.27 mm and of relative permittivity The length a of resonators have been chosen so that a = 16.89 mm at the frequency of 1GHz and the opening gap g of the resonators is 1.5mm.

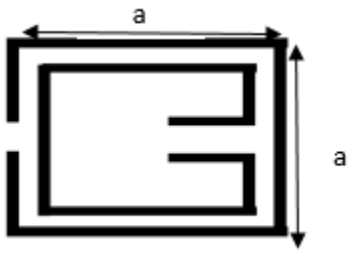

Figure 4: Resonators in split rings with inside a hairpin

3.2. Determination of inter-resonator distances dij

There exist various manners of positioning the resonators the ones compared to the others. The way in which they are positioned and the distances, which separate them, determine the nature and the coupling strong. The electric coupling is of negative sign and it is obtained when the openings of the resonators are opposite one the other (fig.7a). The coupling is magnetic when the opposite sides of the resonators are placed in the vicinity (Fig.7b). When the two resonators are directed as towards the fig. 7c, the two mechanisms of coupling have similar effects and this coupling is known as mixed coupling

a) b) c)

Figure 5: Different coupled SRR structures with a) electric coupling b) magnetic coupling, c) mixed coupling.

To determine the distances between resonators we simulated the circuits of Fig.5a), 5b) and 5c). Each structure is simulated in the frequency range from 0.94 to 1.06 GHz with ADS Momentum. The frequency step is chosen small enough to capture the resonance peak frequencies of the resonators. The values of the electrical, magnetic and mixed coupling coefficients are calculated from (21) [12]

$$K_X = \pm \frac{f_2^2 - f_1^2}{f_2^2 + f_1^2} \quad (21)$$

Where x= E for the electric coupling, x= M for the magnetic coupling and x= B for the mixed coupling

Figures I.6 show the curves of the coupling coefficients obtained. These curves show that the magnetic coupling (K_M) is stronger than the electrical coupling (K_E) and that of the mixed coupling (K_B) lying between the two.

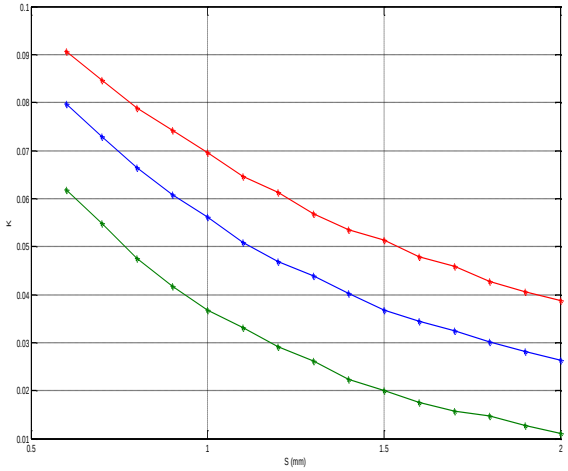

Figure.6: Inter-resonator coupling KE electrical coupling (- - -), KM magnetic coupling (- - -) and KB mixed coupling (- - -)

It remains to determine the coupling coefficients between input and output (I / O) resonators with 50 Ω fed lines. These couplings are intimately related to the external quality factors and are controlled by the t position, as shown in Fig.7, the smaller is t, the closer is the tap line to a resonator virtual ground, resulting in a lower coupling or a larger external quality factor.

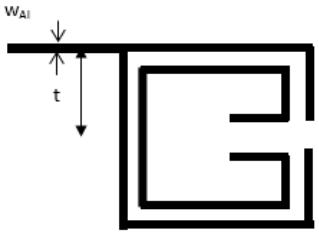

Figure.7: Typical I / O Coupling Structure for Coupled Resonator Filters

To determine the value of t which corresponds to the desired input and output factors quality, we have in a first simulated on ADS Momentum the circuit of figure I.7 by varying t between 0.5 and 1 mm. Fig.8 shows the variation curve of the factor quality of this structure as a function of t.

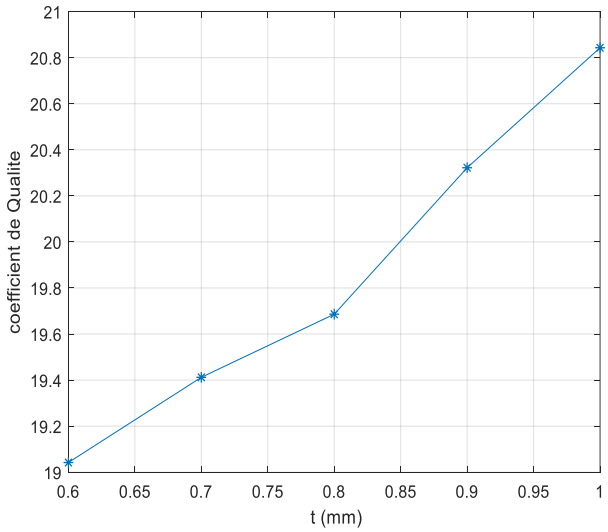

Figure. 8: the curve of variation of the quality coefficient according to t.

In the de-normalized coupling matrix, the coupling coefficient M_{14} has a sign opposite that of the sequential couplings. Therefore, M_{14} will describe the electrical coupling structure. Similarly, the coupling coefficients M_{12} and M_{34} are of positive sign and equal. We opted to represent them by mixed-coupling structures. Finally, the coupling coefficient M_{24} is positive; it has been represented by a magnetic coupling structure.

Table 2 below summarizes all the geometric dimensions of the filter corresponding to the matrix M, deduced from the curves of Fig. 7 and 8.

Table 2: Initial values of the quadruplet filter simulation parameters

Designation	Physical design parame-ter	Calculated dimensions (mm)
Width of the opening gap of resonators	$g_1=g_2=g_3=g_4$	1.5
Resonators length	a	16.89
Resonators width	W	2
Width of feed line	w_{al}	1.48
Position of feed line	t	0.751
Distance resonator 1 – resonator 2	d_{12}	1.46
Distance resonator 1 – resonator 4	d_{14}	1.47
Distance resonator 2 – resonator 3	d_{23}	1.78
Distance resonator 3 – resonator 4	d_{34}	1.46

Once the overall dimensions of this filter are defined, we made its layout as shown in Fig. 9 and then simulated its performance using Momentun ADS

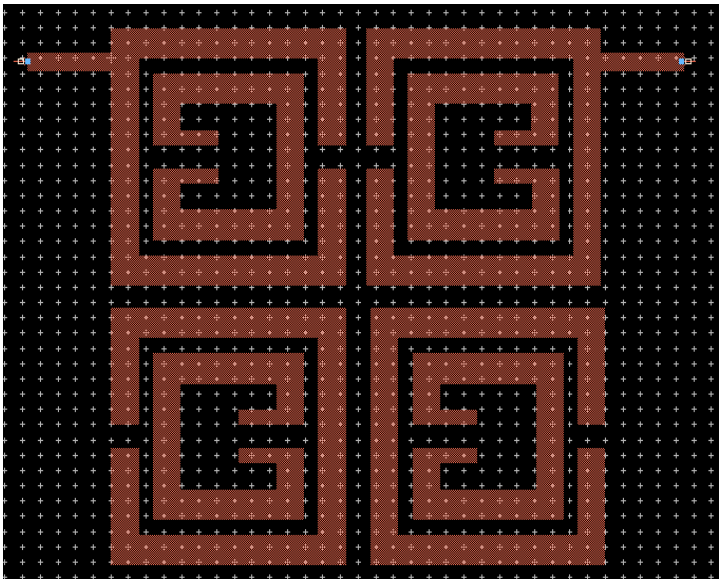

Figure.9: Top view of the structure of a fourth-order SOLR quadruplet filter

Fig.10 shows the frequency response in the [0.94-1.06] GHz range of the optimized bandpass filter which dimensions are given in Table 3.

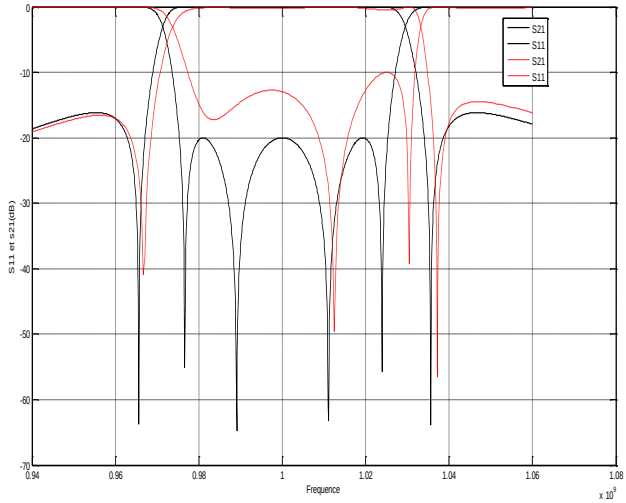

Fig.10: Frequency response of the bandpass filter (-----): simulation curve; (-----) theory curve

As shown in Figure 10, there is good agreement between simulation results over the frequency range of 0.94 to 1.06 GHz and theoretical predictions. The center frequency is about 1 GHz and the bandwidth is about 5.90%, the insertion loss in the bandwidth is 0.464dB

Table 3: Optimized filter dimensions

Designation	Physical design parame-ter	Optimized dimensions (mm)
Width of the opening gap of resonators	$g_1=g_2=g_3=g_4$	1.5
Resonators length	a	16.89
Resonators width	W	2
Width of feed line	w_{al}	1.48
Position of feed line	t	0.811
Distance resonator 1 – resonator 2	d_{12}	1.44
Distance resonator 1 – resonator 4	d_{14}	1.44
Distance resonator 2 – resonator 3	d_{23}	1.78
Distance resonator 3 – resonator 4	d_{34}	1.44

4. CONCLUSION

In this work, we have proposed a new bandpass filter structure with coupled resonators. This structure consists of fused resonators of equal length. We made a design of this filter from a coupled resonator matrix. This design was made using ADS MOMENTUM software. The compact filter obtained has low insertion losses with good selectivity. It can find its application in mobile communications.

References

[1] J. B. Pendry, A. J. Holden, D. J. Robbins, and W. J. Stewart, "Magnetism from conductors and enhanced nonlinear phenomena," IEEE Trans. Microwave Theory Tech., vol. 47, no. 11, pp. 2075-2084, Nov. 1999.

[2] S.-H. Jang and J.-C. Lee, "Design of novel cross-coupling elliptic function filters with the miniaturized edge-coupled split ring resonators," Microwave and Optical Technology Letters, vol. 45, no. 6, pp. 495-499, June 2005.

[3] Z. Troudi, S. Naoui, L. Latrach et L. Osman "Amélioration des performances d'un filtre passe-bande à base d'une nouvelle structure de RAF," Journées Nationales Microondes16-19 mai 2017 – Saint-Malo, France

[4] Armando Fernández-Prieto, Aintzane Lujambio, Ferran Martín, Jesús Martel, Senior, Francisco and Rafael R. Boix, Member "Compact Balanced-to-Balanced Diplexer Based on Split-Ring Resonators Balanced Bandpass Filters" IEEE, microwave and wireless components letters, 2018

[5] R. R. Sushmeetha and S. Natarajamani "Dual-band Bandpass Filter Using Complementary Split Ring Resonators for X-Band Applications", proceeding IEEE,2018

[6] Mohammed Bendaoued, Rachid Mandry, Larbi El Abdellaoui, Aytouna Fouad and Mohamed Latrach "Square Complementary Split Ring Resonator (CSRR) Low Pass Filter", ICCWCS, April 2019

[7] Mohssine El Ouahobi, Alia Zakriti, Mohamed Essaaidi, Aziz Dkiouak "Effect of rotational split ring resonator on dual bandstop filter", pp. 681-686 Elsevier, 2019

[8] Darine Kaddour "Conception et Réalisation de filtres RF passe-bas à structures périodiques et filtres Ultra Large Bande, semi-localisés en technologie planaire", thèse doctorat, Université Joseph-Fourier-Grenoble, 28 Mar 2008

[9] A.E. Atia and A.E. Williams, "Narrow -bandpass waveguide filters," IEEE Trans. Microwave Theory Tech., vol. MTT-20, pp.258-265, April 1972.

[10] R. J. Cameron," General coupling matrix synthesis methods for Chebychev filtering functions, " IEEE Trans. Microwave Theory Tech., vol. MTT-47, pp. 433-442, April.1999.

[11] R.J. Cameron, "Advanced coupling matrix synthesis techniques for microwave filters," IEEE Trans. Microwave Theory Tech., vol.MTT-51, pp.1-10, January 2003.

[12] Matthias CAENEPEEL, " Modeling technique for the efficient design of microwave bandpass filters" these doctoral, universite de nice Sophia Antipolis, 19 October 2016